IEEE Access
Multidisciplinary | Rapid Review | Open Access Journal

Received October 24, 2020, accepted November 3, 2020, date of publication November 9, 2020, date of current version November 19, 2020.

Digital Object Identifier 10.1109/ACCESS.2020.3036724

Improved PWM-OFF-PWM to Reduce Commutation Torque Ripple of Brushless DC Motor Under Braking Conditions

QIXUN ZHOU, JIANHUA SHU, ZIWEI CAI, QUANLONG LIU, AND GUANGHUI DU
School of Electrical and Control Engineering, Xi'an University of Science and Technology, Xi'an 710054, China

Corresponding author: Jianhua Shu (19206029023@stu.xust.edu.cn)

This work was supported in part by the Doctoral (Postdoctoral) Research Initiation Fund Project of Xi'an University of Science and Technology (14QDJ08), and in part by the Natural Science Basic Research Program of Shaanxi-Shanmei Joint Fund under Grant Program (2019JLM-51).

ABSTRACT This paper proposes an improved PWM-OFF-PWM of the brushless DC motor under braking condition which can reduce commutation torque ripple. Compared with other brake modulation methods, PWM-OFF-PWM can restrain non-commutation torque ripple attributed to non-conductive freewheeling, while incapable of suppressing commutation torque ripple at low speeds effectively. Therefore, to solve commutation torque ripple caused by the turn-off time being shorter than turn-on time, an improved PWM-OFF-PWM is proposed in this paper. Moreover, to describe the influence factors of commutation torque ripple, the formulas of the duty cycle of switching tube in the commutation period and that during non-commutation period is derived. We can conclude from mathematical analysis that when duty cycles of outgoing and incoming phases satisfy derived formula, the non-commutation current in commutation interval will be more stable, which can contribute to suppress the commutation torque ripple at low speed under PWM-OFF-PWM mode and to improve the operation stability of BLDCM. The correctness and feasibility of the proposed method can be proved by simulation and experimental results.

INDEX TERMS Brushless DC motor, braking operation, commutation torque ripple, improved PWM-OFF-PWM.

I. INTRODUCTION

Brushless DC motor (BLDCM), as characterized by high efficiency, large density of power, and convenient control, has been widely applied in electric vehicle, industrial, and medical equipment [1], [2]. Nevertheless, the torque ripple, in particular, the commutation torque ripple attributed to the structure characteristics and commutation method, has restricted the use prospect of BLDCMs in fields with high performance.

In motoring operation, numerous studies are conducted on the reduction of commutation torque ripple, with the suppression strategies being roughly classified as three categories below:

1) Equalize various change rates of the currents of the incoming and outgoing phases in the interval of the commutation [3]–[9]. In order to achieve the goal of restraining commutation torque ripple, different control strategies are studied: The pulse width modulation (PWM) method for commutation interval is proposed [3]–[5]. A torque ripple suppression control method based on current predictive control strategy is proposed in [6], [7]. In [8] and [9], the multimode current hysteresis control and deadbeat current control scheme are used respectively.

2) Alter the DC bus voltage to maintain a specific proportional relationship with the back EMF during the commutation period [10]–[14]. In order to suppress commutation torque ripple, single-ended primary inductor converter, cuk converter, Z-Source inverter, and auxiliary Step-Up circuit are introduced in these literatures.

3) Control the instantaneous electromagnetic torque [15]–[20]. Among them, the torque control strategies can reduce torque ripple of BLDCM with nonideal back electromotive force in [15]–[17]. The improved direct torque

The associate editor coordinating the review of this manuscript and approving it for publication was Kan Liu.

control (DTC) scheme is proposed in [18], [19]. A novel commutation analysis method of the BLDCM based on coordinate transformation theory is proposed in [20].

Braking condition refers to an operating condition of the BLDCM relative to motor condition, which cannot be ignored. In braking operation, the variation trend and the circuit of the current are more diverse from those in motor operation. However, the braking operation also faces the problem of commutation torque ripple.

The research on braking operation is introduced in [21]–[31]. To achieve dual objectives of braking and energy recovering process, a variety of hybrid energy storage systems, such as supercapacitor + DC-DC converter in regenerative braking system, are proposed in [21]–[23]. In [24], regenerative braking is realized by adopting H_PWM-L_PWM modulation mode, based on which, [25] compares the application speed range of the existing plug and regenerative braking modulation methods, and finally proposes a new method based on H_PWM-L_PWM capable of suppressing commutation torque ripple in the full speed range is proposed. To reduce the times of switching, [26] illustrates one new regenerative braking control approach based on the unipolar H_OFF-L_PWM mode, but the torque ripple is not considered in this paper. According to torque control performance of each modulation mode with different speed range, a torque control strategy, which combines plug and regenerative braking modulation is proposed in [27], [28]. The regenerative ability of braking energy based on bipolar and unipolar modulating conditions is compared in [29], and concludes that the regenerative capacity of braking energy in unipolar mode is better than that in bipolar mode. In addition, a new braking PWM strategy, termed as PWM-OFF-PWM, is proposed in [30], [31], which can eliminate the diode freewheeling of the non-commutation phase during the non-commutation period under the braking condition of BLDCM.

As we can see, researches on braking operation mainly focus on energy recovery and torque ripple in the interval of normal conduction, while there is little focus on commutation torque ripples.

The electrical braking mode of BLDCM is divided into plug and regenerative braking modulation. Compared with plug braking, the braking current of regenerative braking can be provided by the motor itself, and at the same time, the electric energy can be fed back to the battery, which is not only economical and environmentally friendly, but also prolongs the battery life. Therefore, regenerative braking has a good development prospect. In order to suppress commutation torque ripple, the commonly used methods include modulation method, current prediction method, and introducing new link to adjust DC bus voltage to maintain a specific proportional relationship with back EMF. Compared with the modulation method, other methods not only introduce new algorithms to increase the complexity of the system, but also may rely too much on accurate motor parameters and models. In addition, compared with other regenerative braking modulation methods, PWM-OFF-PWM can restrain non-commutation torque ripple attributed to non-conductive freewheeling, while incapable of suppressing commutation torque ripple at low speeds effectively.

In this paper, an improved PWM-OFF-PWM is proposed to suppress the commutation torque ripple for BLDCM in the braking state. Contributions of this article are as follows: 1) Problems and reasons existing in the traditional PWM-OFF-PWM modulation method are analyzed. 2) An improved PWM-OFF-PWM is proposed to solve commutation torque ripple caused by turn-off time being shorter than turn-on time. 3) According to the mathematical analysis, we can draw the conclusion that when duty cycles of the outgoing and incoming phases meet the derived formula at commutation stage, the sudden change of non-commutation current will effectively suppress, inhibiting the commutation torque ripple under PWM-OFF-PWM mode and improving the operating stability of BLDCM.

The rest of this paper is organized as follows: First, Section II illustrates the cause of commutation torque ripple under the traditional PWM-OFF-PWM modulation, followed by the introduction of the improved PWM-OFF-PWM modulation in Section III. In Section IV, simulation and experimental verification of the proposed method are performed, ending up with the conclusion summarized in Section V.

II. CAUSE OF COMMUTATION TORQUE RIPPLE BASED ON TRADITIONAL PWM-OFF-PWM MODULATION

A. MATHEMATICAL MODEL OF BLDCM

Assume the armature reaction and the losses of eddy currents and hysteresis are negligible. Fig.1 illustrates the equivalent circuit of BLDCM with symmetrical three-phase windings.

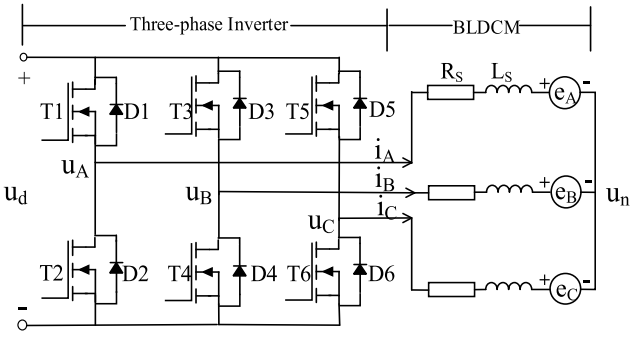

FIGURE 1. Equivalent circuit of BLDCM.

The voltage equations are described as:

$$\begin{cases} u_A = Ri_A + L_S\dfrac{di_A}{dt} + e_A + u_n \\ u_B = Ri_B + L_S\dfrac{di_B}{dt} + e_B + u_n \\ u_C = Ri_C + L_S\dfrac{di_C}{dt} + e_C + u_n \end{cases} \tag{1}$$

where i_k, u_k, and $e_k(k \in A, B, C)$ respectively denote the phase current, terminal voltage, and back EMF; u_n represents

the neutral point voltage; R_S and L_S respectively represent the phase resistance and phase inductance; u_d denotes the DC bus voltage.

BLDCM electromagnetic torque is:

$$T_e = \frac{i_A e_A + i_B e_B + i_C e_C}{\omega} \tag{2}$$

where ω denotes the mechanical angular velocity.

The three-phase current equation of BLDCM with the star-connected stator windings is:

$$i_A + i_B + i_C = 0 \tag{3}$$

Taking no account of the magnetic saturation, the amplitude of phase back EMF is:

$$E = k_e \omega \tag{4}$$

where k_e denotes the phase back EMF coefficient.

B. TRADITIONAL PWM-OFF-PWM MODULATION

Five typical braking modulation strategies of BLDCM are OFF-PWM, PWM-OFF, H_OFF-L_PWM, H_PWM-L_ OFF, and PWM-OFF-PWM modulation, to be specific, PWM-OFF-PWM is the only one which does not have diode freewheeling of the non-commutation phase during the normal conduction period. And the modulation waveform of PWM-OFF-PWM is illustrated in Fig.2, where θ denotes the electrical angular.

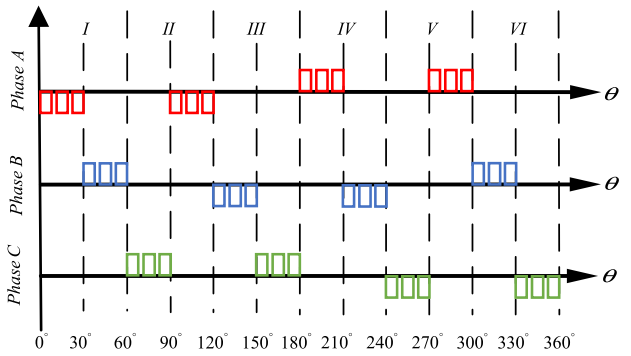

FIGURE 2. PWM-OFF-PWM modulation waveform.

To analyze the reason for the commutation torque ripple, the 60° commutation moment is considered. In this commutation interval, phase A, B, and C is non-commutation, outgoing, and incoming phase separately.

Equivalent circuit of the commutation in the 60° moment is shown in Fig.3, where the dotted line represents actual directions of currents. When PWM = ON, phase C current flows via the switch T5, as shown in Fig.3 (a). And when PWM = OFF, the current of phase C flows via the diode D6, as shown in Fig.3 (b).

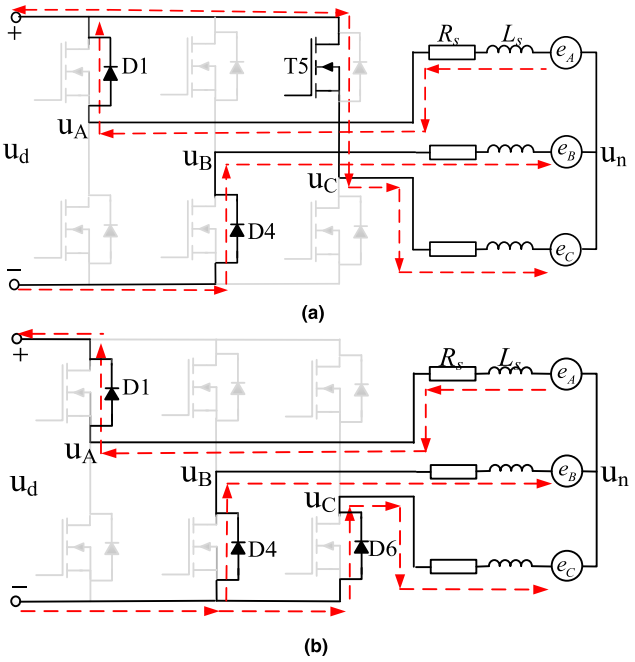

FIGURE 3. Equivalent circuit of the commutation process at 60° commutation time under PWM-OFF-PWM mode. (a) PWM = ON. (b) PWM = OFF.

The formulas of three-phase terminal voltage are:

$$\begin{cases} u_A = u_d = Ri_A + L_S \dfrac{di_A}{dt} + e_A + u_n \\ u_B = 0 = Ri_B + L_S \dfrac{di_B}{dt} + e_B + u_n \\ u_C = Du_d = Ri_C + L_S \dfrac{di_C}{dt} + e_C + u_n \end{cases} \tag{5}$$

where D denotes duty cycle of the switch.

For a significantly short PWM period, the back EMF of outgoing phase B is regarded to be constant. In this commutation interval, the back EMF satisfies $e_A = -e_B = -e_C = E$, and the phase current meets $-i_A = i_B = I$. Taking no account of the stator resistance voltage, the relationship of the current and time during the commutation is as follows:

$$\begin{cases} i_A = -I + \dfrac{(2-D)\,u_d - 4E}{3L_S}\Delta t \\ i_B = I + \dfrac{-(1+D)\,u_d + 2E}{3L_S}\Delta t \\ i_C = \dfrac{(2D-1)\,u_d + 2E}{3L_S}\Delta t \end{cases} \tag{6}$$

Comparing the electromagnetic torque before and after the commutation process, the expression of the torque ripple at the commutation time 60° is solved as:

$$\Delta T = \frac{(4-2D)\,u_d E - 8E^2}{3L_S \omega}\Delta t \tag{7}$$

Similarly, the expressions of torque ripple at other commutation times are analyzed, and it is found that the analytical formula of torque ripple at each commutation time is the

same. Substitute (4) into (7) and make it equal to 0, the duty cycle is subsequently yielded:

$$D = 2 - \frac{4k_e\omega}{u_d} \tag{8}$$

The following relationship is satisfied in the BLDCM:

$$\begin{cases} 0 \le D \le 1 \\ 0 \le \omega \le \omega_N \\ u_d = U_N = 2RI_N + 2k_e\omega_N \end{cases} \tag{9}$$

where U_N, I_N, and ω_N represent the rated voltage, current, and mechanical angular velocity respectively.

Then under traditional PWM-OFF-PWM modulation pattern, the speed range in which commutation torque ripple is suppressed refers to:

$$\frac{u_d}{4k_e} \le \omega \le \omega_N \tag{10}$$

Remark 1: Based on the above analysis, if the PWM-OFF-PWM duty can satisfy range in (10), the commutation torque ripple can be suppressed. However, when $u_d > 4k_e\omega (u_d > 4E)$, the commutation torque ripple cannot be reduced.

C. COMPARISON OF DIFFERENT COMMUTATION PROCESSES

The current flowing from phase B to Phase C is analyzed as a case for illustrating the commutation process, in which phase A refers to the non-commutation phase. Fig.4 presents the relationship among back EMF, DC bus voltage, and current under PWM-OFF-PWM mode.

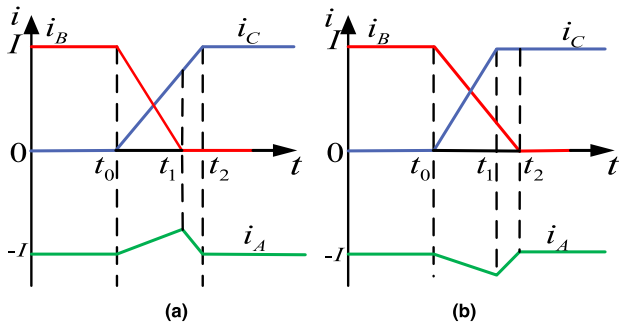

FIGURE 4. Current waveform of each phase in the course of commutation at different speeds. (a) $u_d > 4E$. (b) $u_d < 4E$.

As shown in Fig.4 (a), under $u_d > 4E$ of low speed, the change rate of the outgoing phase reaches over that of the incoming phase. Under $u_d > 4E$ of high speed, the change rate of two phases is opposite to the low speed situation in Fig.4 (b).

Remark 2: The current of the non-commutation phase changes during the commutation period due to the unequal current change rate of the outgoing and incoming phases, resulting in torque ripple.

D. OBJECTIVE EQUATION FOR CONTROLLING COMMUTATION TORQUE RIPPLE

Next, the commutation process will be explained by taking the commutation in the 60° moment as an example, and the phase A is non-commutation. And the back EMF satisfies $e_A = -e_B = -e_C = E$. By substituting (3) together with (4) into (2), the electromagnetic torque is:

$$T_e = \frac{E(i_A - i_B - i_C)}{\omega} = 2k_e i_A \tag{11}$$

Torque ripple is equal to the difference between instantneous electromagnetic torque and steady-state value, which can be expressed as:

$$\Delta T_e = T_e - T_e^* = 2k_e \Delta i_A \tag{12}$$

where T_e^* is the steady-state electromagnetic torque of the non-commutation interval before the corresponding commutation time.

It can be seen from (12) that the commutation torque ripple is proportional to the ripple of non-commutation current. Therefore, commutation torque ripple can be controlled by non-commutation current in commutation interval:

$$\Delta i_A = \frac{di_A}{dt} = 0 \tag{13}$$

Lemma 1: The commutation torque ripple can be reduced when the change rate of non-commutation current in commutation interval reaches 0.

III. PROPOSED IMPROVED PWM-OFF-PWM MODULATION

Based on the analysis above, it can be seen that equalizing the different change rate of the incoming and outgoing phase currents in the commutation interval is a necessary and sufficient condition to eliminate torque ripple.

However, PWM-OFF-PWM cannot adjust the duty cycle for suppressing commutation torque ripple when the decrease ratio of the outgoing phase reaches over the increase ratio of the incoming phase.

Therefore, this paper proposes an improved PWM-OFF-PWM, which aims to extend the turn-off time and shorten the turn-on time. Finally realize that these two kinds of time can be equal during commutation. Fig.5 gives the schematic figure of commutation:

In which D denotes the duty cycle of the switch modulation during non-commutation period. In the commutation interval, the outgoing and incoming phases are chopped with duty cycle D_{off} and D_{on} respectively. The relationship between three duty cycles is: $D_{off} < D < D_{on}$. The commutation time is determined by dynamic detection of if the outgoing phase current is down-regulated to 0.

During PWM modulation, Fig.6 gives the three-phase modulation schematic diagram of the commutation process from AB to AC. At this time the outgoing, incoming phase, and non-commutation phase correspond to the conduction of T3, T5 and D1 respectively. The entire modulation cycle can

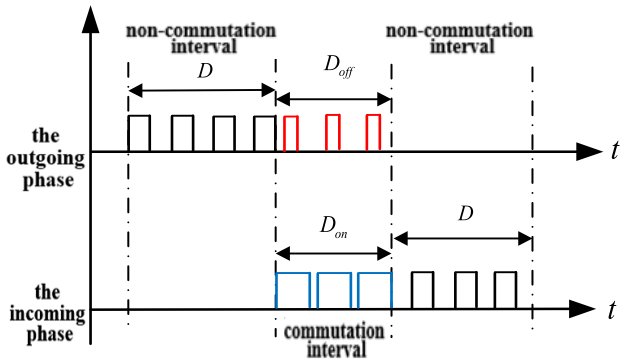

FIGURE 5. Improved overlapping commutation diagram.

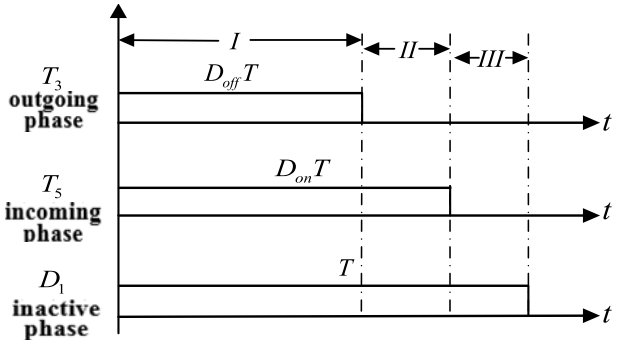

FIGURE 6. Commutation interval modulation diagram.

be divided into three stages, which have been marked in the figure.

A. SECTION I OF COMMUTATION INTERVAL

T3, T5, and D1 are all on in the section I of commutation interval, and the state diagram is shown in Fig.7.

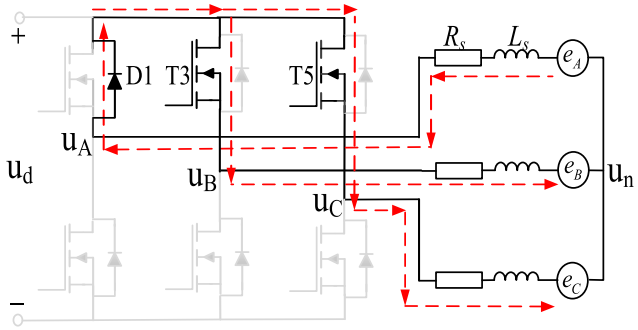

FIGURE 7. Section I diagram.

The three phase terminal voltage expressions are:

$$\begin{cases} u_A = 0 = Ri_A + L_S\dfrac{di_A}{dt} + e_A + u_n \\ u_B = 0 = Ri_B + L_S\dfrac{di_B}{dt} + e_B + u_n \\ u_C = 0 = Ri_C + L_S\dfrac{di_C}{dt} + e_C + u_n \end{cases} \tag{14}$$

And the back EMF satisfies $e_A = -e_B = -e_C = E$, substituting (3) into (14), the neutral point voltage u_n is:

$$u_n = \frac{E}{3} \tag{15}$$

Taking no account of the stator resistance voltage, the current change rate of three-phase during section I is as follows:

$$\begin{cases} i'_{AI} = -\dfrac{4E}{3L_S} \\ i'_{BI} = \dfrac{2E}{3L_S} \\ i'_{CI} = \dfrac{2E}{3L_S} \end{cases} \tag{16}$$

B. SECTION II OF COMMUTATION INTERVAL

T5 and D1 are open in the section II of commutation interval, and the diagram is shown in Fig.8.

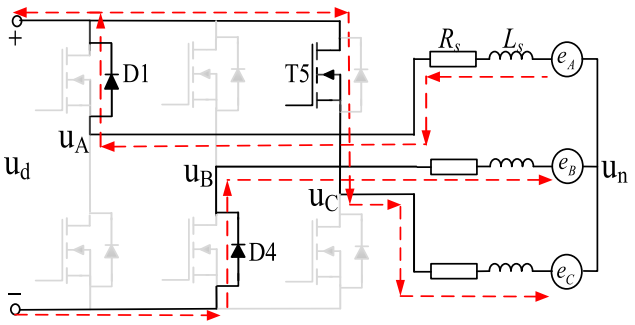

FIGURE 8. Section II diagram.

According to the same analysis method, the change ratio of three-phase current in the section II as follows:

$$\begin{cases} i''_{AII} = \dfrac{u_d - 4E}{3L_S} \\ i''_{BII} = \dfrac{-2u_d + 2E}{3L_S} \\ i''_{CII} = \dfrac{u_d + 2E}{3L_S} \end{cases} \tag{17}$$

C. SECTION III OF COMMUTATION INTERVAL

D1 is in the on state during the section III of commutation interval, and the diagram is shown in Fig.9.

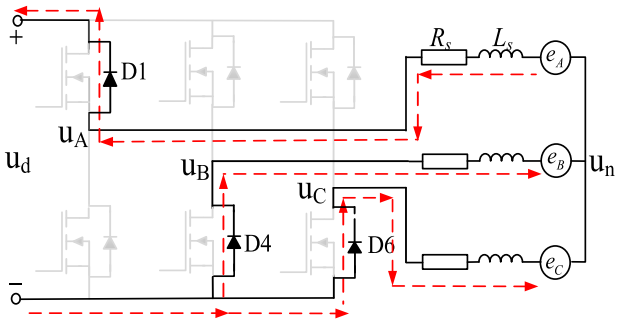

FIGURE 9. Section III diagram.

In section III, the current change rate of three-phase is:

$$\begin{cases} i'''_{AIII} = \dfrac{2u_d - 4E}{3L_S} \\ i'''_{BIII} = \dfrac{-u_d + 2E}{3L_S} \\ i'''_{CIII} = \dfrac{-u_d + 2E}{3L_S} \end{cases} \tag{18}$$

During a commutation period, the average change ratio of three-phase current is:

$$\overline{i'_k} = D_{off} i'_{kI} + (D_{on} - D_{off}) i''_{kII} + (1 - D_{on}) i'''_{kIII} (k \in A, B, C) \tag{19}$$

Substituting (16)-(18) into (19), the current change rate of three-phase in a PWM cycle is as follows:

$$\begin{cases} \overline{i'_A} = \dfrac{[2 - (D_{on} + D_{off})]u_d - 4E}{3L_S} \\ \overline{i'_B} = \dfrac{-(1 + D_{on})u_d + 2E}{3L_S} \\ \overline{i'_C} = \dfrac{(2D_{on} - D_{off} - 1)u_d + 2E}{3L_S} \end{cases} \tag{20}$$

For the two-phase conduction BLDCM, the following condition is satisfied:

$$Du_d = 2E \tag{21}$$

The torque is proportionally related to the non-commutation phase current in the course of commutation. Therefore, the commutation torque ripple is able to be suppressed if the average change rate of non-commutation phase A current reaches 0 in commutation. In summary, the relationship between the three duty cycles is as follows:

$$D_{on} + D_{off} = 2(1 - D) \tag{22}$$

Lemma 2: To delay the change rate of the outgoing phase current, $D_{off} < D < D_{on}$ should be ensured at the same time. In conclusion, the torque ripple can be suppressed as long as (22) is satisfied in the commutation interval.

D. DETERMINATION OF COMMUTATION TIME

The previous article discussed the determination of the duty cycle of each phase PWM modulation. In addition, it is also necessary to know the duration of the commutation process. Based on the above analysis, the commutation specific duty cycle time is composed of several modulation cycles, and the ideal state is that when the commutation ends, the outgoing phase current just reaches 0. Define the commutation time as t_0, then:

$$\begin{cases} T \cdot f = 1 \\ t_0 = nT \\ \left|\overline{i'_B}\right| \times t_0 = I \end{cases} \tag{23}$$

where f is the switching frequency. And the commutation time is:

$$t_0 = nT = \frac{3IL_S}{(1 + D_{on} - D)u_d} \tag{24}$$

In summary, the duty cycles of outgoing and incoming phases satisfies (22), and the action time $t = t_0$, the non-commutation current can be kept stable during commutation period, thereby suppressing the commutation torque ripple.

IV. SIMULATION AND EXPERIMENTAL RESULTS

The improved PWM-OFF-PWM is proved to be correct and feasible by simulating and experimenting.

A. SIMULATION RESULTS

The BLDCM braking system adopts double closed-loop control approach of speed and current. Table 1 lists the main parameters of BLDCM.

TABLE 1. Main parameters of BLDCM.

Motor parameters	Value	Unit
DC bus voltage	310	V
Pole pairs	2	
Phase resistance	4.765	Ω
Phase inductance	0.0085	H
Rated speed	3000	r/min
Rated torque	2.5	*N•m*
Phase back EMF coefficient	0.349	V/(rad/s)

Take the commutation process from phase B to C as a case for analysis, in which B denotes the outgoing phase, C refers to the incoming phase, and A indicates the non-commutation phase.

When the duty cycle $D = 0.5$, the three-phase current waveforms under the ordinary and improved PWM-OFF-PWM method are shown in Fig.10 (a) and (b), separately.

In order to meet the requirements of $D_{on} + D_{off} = 2(1 - D)$ and $D_{off} < D < D_{on}$, the duty cycles of incoming and outgoing phase under the improved PWM-OFF-PWM method are selected as $D_{on} = 0.8$ and $D_{off} = 0.2$ respectively.

Comparing Fig.10 (a) and (b), it can be found that under the PWM-OFF-PWM method, the current change rate of the outgoing and the incoming phases is inconsistent and the former has a larger change rate than the latter, which causes current fluctuations in non-commutation phase, causing commutation torque ripple.

With the improved PWM-OFF-PWM proposed in this paper, the decreasing ratio of outgoing phase current equals to the increasing ratio of incoming phase current, and the non-commutation current is basically stable in the process of current commutation.

Fig.11 (a) and (b) respectively present the electromagnetic torque waveforms under the above two methods.

Comparing results shown in Fig.11, we can see the electromagnetic torque waveform of Fig.11 (b) is more stable than that of Fig.11 (a) during commutation. Therefore, the

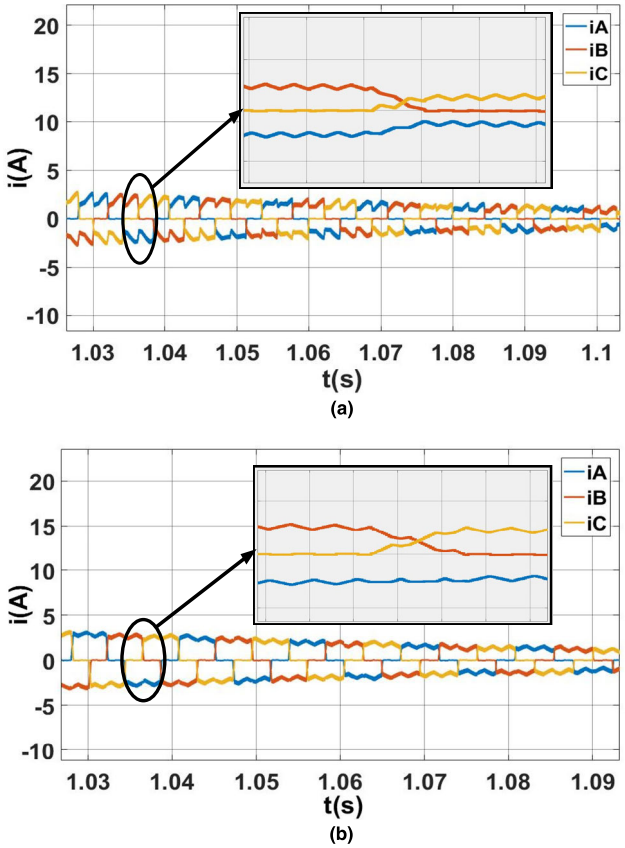

FIGURE 10. Waveform of current simulation under two methods when D = 0.5. (a) ordinary PWM-OFF-PWM. (b) improved PWM-OFF-PWM.

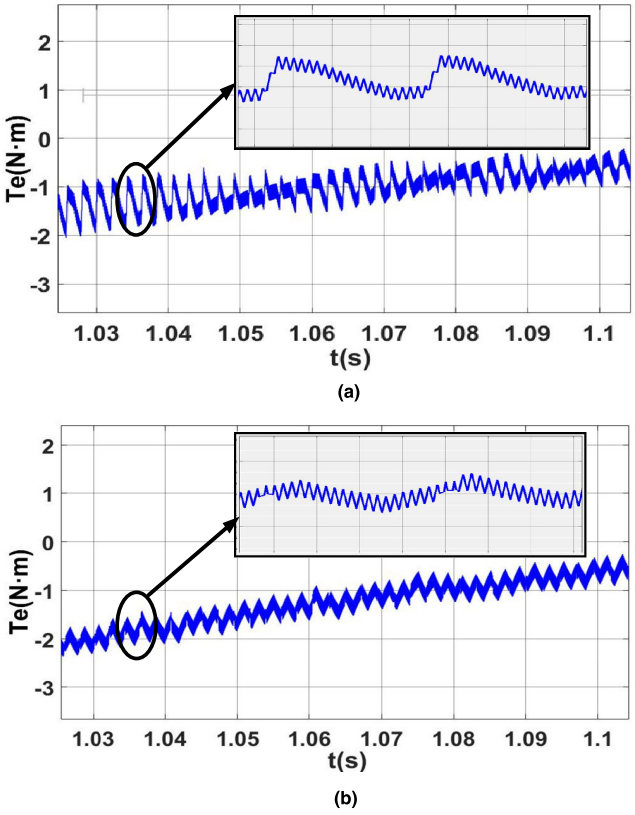

FIGURE 11. Waveform of electromagnetic torque simulation under two methods when D = 0.5. (a) ordinary PWM-OFF-PWM. (b) improved PWM-OFF-PWM.

improved PWM-OFF-PWM proposed in this paper can effectively suppress commutation torque ripple.

When the duty cycle $D = 0.5$, Fig.12 (a) and (b) show the waveforms of drive signals of power switches T3 and T5, three-phase current, and torque under two modulation modes.

According to Fig.12, when ordinary PWM-OFF-PWM is commutating from AB to AC, the upper bridge arm T5 of phase C is on with duty cycle D, and the upper bridge arm T3 of phase B is disconnected at the beginning of commutation. While the improved PWM-OFF-PWM is commutating, the switch T5 is turned on with duty cycle D_{on}, and T3 is turned on continuously during commutation.

As shown in Fig.12, the torque ripples before and after the improvement of PWM-OFF-PWM is 0.22 $N \cdot m$ and 0.83 $N \cdot m$, respectively, and the improvement is reduced by 73.49% compared with the traditional one. It is found that the decrease rate of outgoing phase current is slowed down, while the increase rate of incoming phase current is increased appropriately, which makes the change rate of the two methods basically the same, and the torque ripple in commutation interval is also significantly weakened.

The torque ripples at different speeds are obtained by the ordinary and improved PWM-OFF-PWM, as shown in Table 2. In this analysis, the duty cycle $D = 0.5$, $D_{on} = 0.8$, and $D_{off} = 0.2$ respectively, and the commutation from AB to AC phase is selected.

TABLE 2. The commutation torque ripples at various speeds.

Number	Speed (r/min)	Commutation torque ripple ($N\cdot m$)	
		Ordinary PWM-OFF-PWM	Improved PWM-OFF-PWM
1	2500	0.9142	0.3021
2	2200	0.8955	0.2959
3	1900	0.7301	0.2239
4	1600	0.4979	0.2111
5	1300	0.2507	0.2018
6	1000	0.2129	0.1865
7	700	0.1795	0.1524
8	400	0.1101	0.0899

It can be seen from Table 2 that the commutation torque ripple of the improved PWM-OFF-PWM is smaller than that of the ordinary PWM-OFF-PWM at any speed.

B. EXPERIMENTAL RESULTS

For in-depth verification of the strategy proposed here, the experimental platform as shown in Fig.13 is built. The controller complies with the DSP of TMS320F28335, and the parameters of the BLDCM are the same as simulation.

(1) Experiments with different duty cycle D_{on} and D_{off} under the same duty cycle D

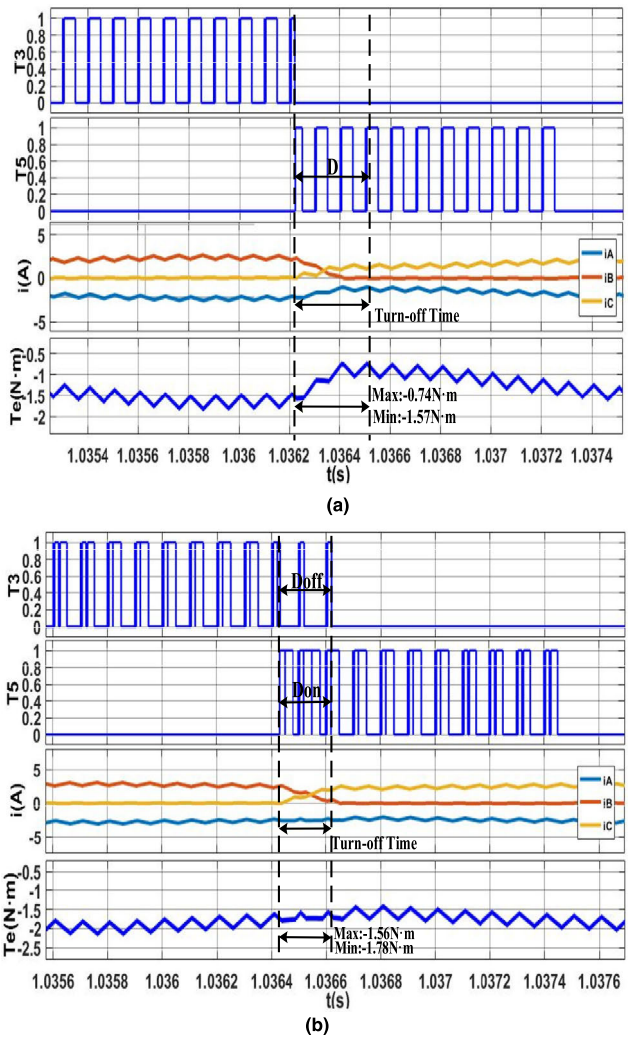

FIGURE 12. Waveform of state of T3 and T5, current, and electromagnetic torque simulation under two methods when D = 0.5. (a) ordinary PWM-OFF-PWM. (b) improved PWM-OFF-PWM.

In order to prove that under different duty cycle D_{on} and D_{off} under the same duty cycle D, the torque ripple suppression effect of ordinary PWM-OFF-PWM can be improved as long as the proposed requirements are met. Therefore, when the duty cycle $D = 0.5$, in order to meet the requirements of (22), the duty cycles of incoming and outgoing phase under the improved PWM-OFF-PWM method should meet the equation $D_{on} + D_{off} = 2(1 - D) = 1$ and $D_{off} < D < D_{on}$, then three groups of comparative experiments are selected as: ① $D_{on} = 0.6$ and $D_{off} = 0.4$; ② $D_{on} = 0.8$ and $D_{off} = 0.2$; ③ $D_{on} = 0.9$ and $D_{off} = 0.1$ respectively.

It is deduced that the commutation torque ripple is proportional to the pulsation of the non-commutation current, so the ripple of the non-commutation current during the commutation period can be used to replace the commutation torque ripple.

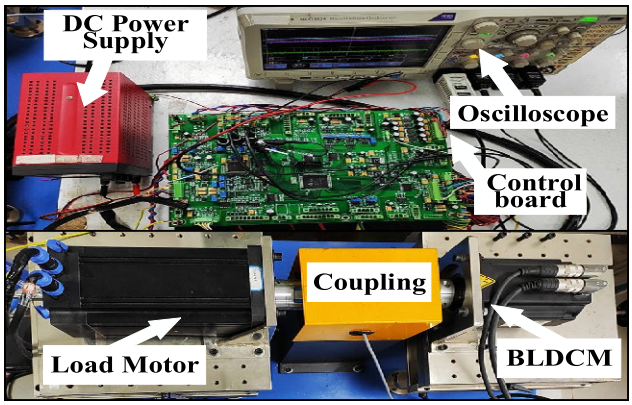

FIGURE 13. Platform of BLDCM experimental system.

1) ORDINARY PWM-OFF-PWM

When the duty cycle $D = 0.5$, the three-phase current waveforms under the ordinary PWM-OFF-PWM method is shown in Fig.14.

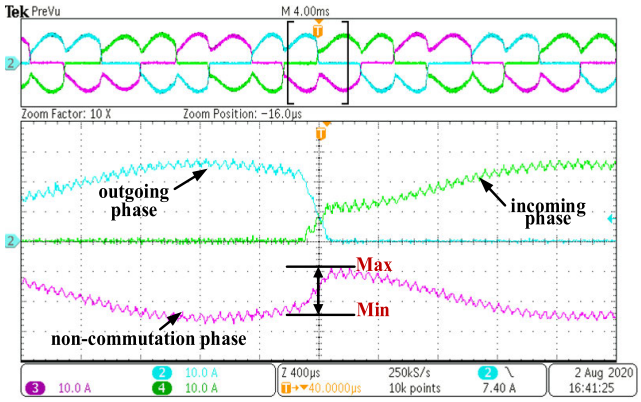

FIGURE 14. Experimental waveform of current under ordinary PWM-OFF-PWM ($D = 0.5$).

It can be found from Fig.14 that under the ordinary PWM-OFF-PWM method, the current change rate of the outgoing and the incoming phases is inconsistent and the former has a larger change rate than the latter, which causes current fluctuations in non-commutation phase, causing commutation torque ripple.

2) IMPROVED PWM-OFF-PWM

① $D_{on} = 0.6$ and $D_{off} = 0.4$

When the duty cycle $D = 0.5$, $D_{on} = 0.6$, and $D_{off} = 0.4$ res-pectively, the three-phase current waveforms under the improved PWM-OFF-PWM method is shown in Fig.15.

Comparing Fig.14 and Fig.15, it can be found that compared with the ordinary PWM-OFF-PWM method, the non-commutation current fluctuation is reduced, indicating that the improved PWM-OFF-PWM can effectively suppress the commutation torque ripple.

② $D_{on} = 0.8$ and $D_{off} = 0.2$

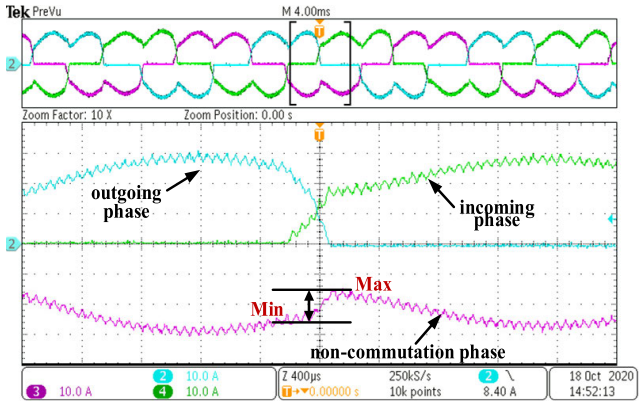

FIGURE 15. Experimental waveform of current under improved PWM-OFF-PWM ($D = 0.5$, $D_{on} = 0.6$, and $D_{off} = 0.4$).

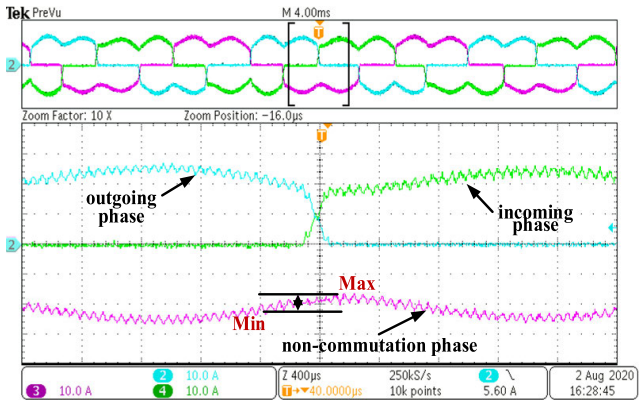

FIGURE 16. Experimental waveform of current under improved PWM-OFF-PWM ($D = 0.5$, $D_{on} = 0.8$, and $D_{off} = 0.2$).

When the duty cycle $D = 0.5$, $D_{on} = 0.8$ and $D_{off} = 0.2$ respectively, the three-phase current waveforms under the improved PWM-OFF-PWM method is shown in Fig.16.

Comparing Fig.14 and Fig.16, it shows that the improved PWM-OFF-PWM can effectively suppress the commutation torque ripple.

③ $D_{on} = 0.9$ and $D_{off} = 0.1$

When the duty cycle $D = 0.5$, $D_{on} = 0.9$ and $D_{off} = 0.1$ respectively, the three-phase current waveforms under the improved PWM-OFF-PWM method is shown in Fig.17.

Under all the current waveform diagrams, different D_{on} and D_{off} have different effects on commutation torque ripple under the same D. But compared with ordinary PWM-OFF-PWM, as long as the duty cycles of the outgoing and the incoming phases in improved PWM-OFF-PWM are satisfied (22), the phenomenon of non-commutation phase current drop in the commutation region is able to be effectively improved, which verifies that the proposed theory is capable of significantly suppressing commutation torque ripple.

(2) Experiments with different duty cycles D

In order to prove that under different duty cycles D, the torque ripple suppression effect of ordinary PWM-OFF-PWM can be improved as long as the proposed

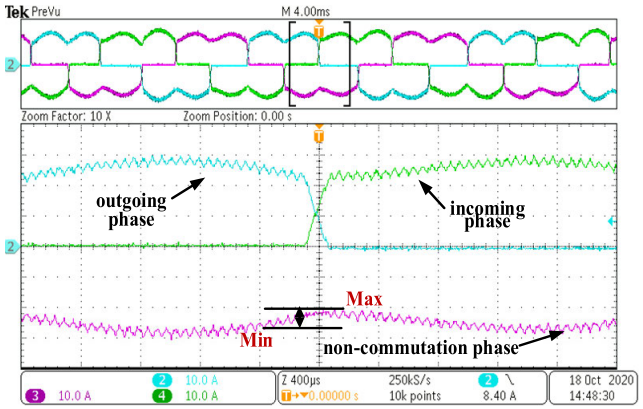

FIGURE 17. Experimental waveform of current under improved PWM-OFF-PWM ($D = 0.5$, $D_{on} = 0.9$, and $D_{off} = 0.1$).

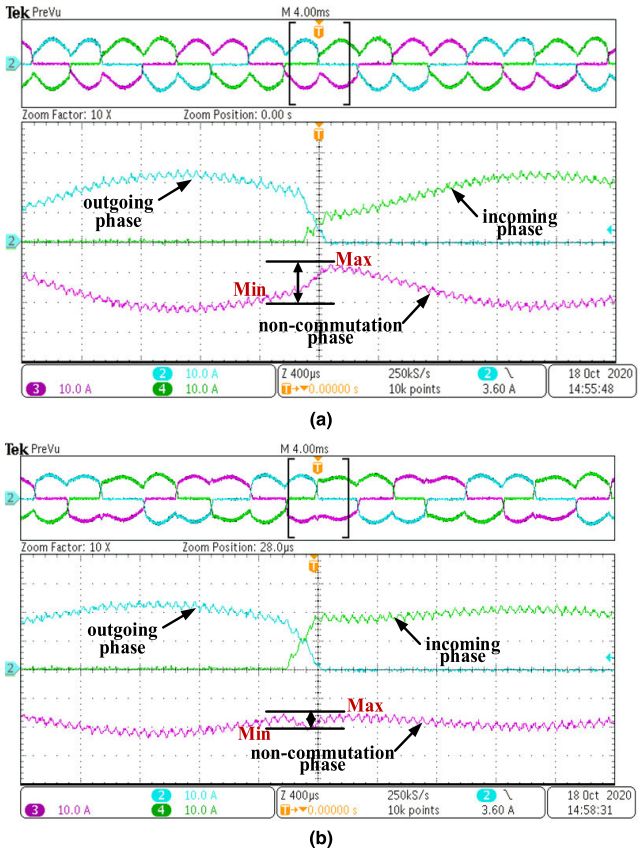

FIGURE 18. Experimental waveform of current under two methods when D = 0.4. (a) ordinary PWM-OFF-PWM. (b) improved PWM-OFF-PWM.

requirements are met. Therefore, the duty cycles of incoming and outgoing phase under the improved PWM-OFF-PWM method should meet the equation $D_{on} + D_{off} = 2(1-D)$, $D_{off} < D < D_{on}$, and $D_{off}, D, D_{on} \in [0, 1]$, the value of the duty cycle D should not be too large or too small. Then three groups of comparative experiments are selected as: ① $D = 0.4$; ② $D = 0.5$; ③ $D = 0.6$ respectively.

1) $D = 0.4$

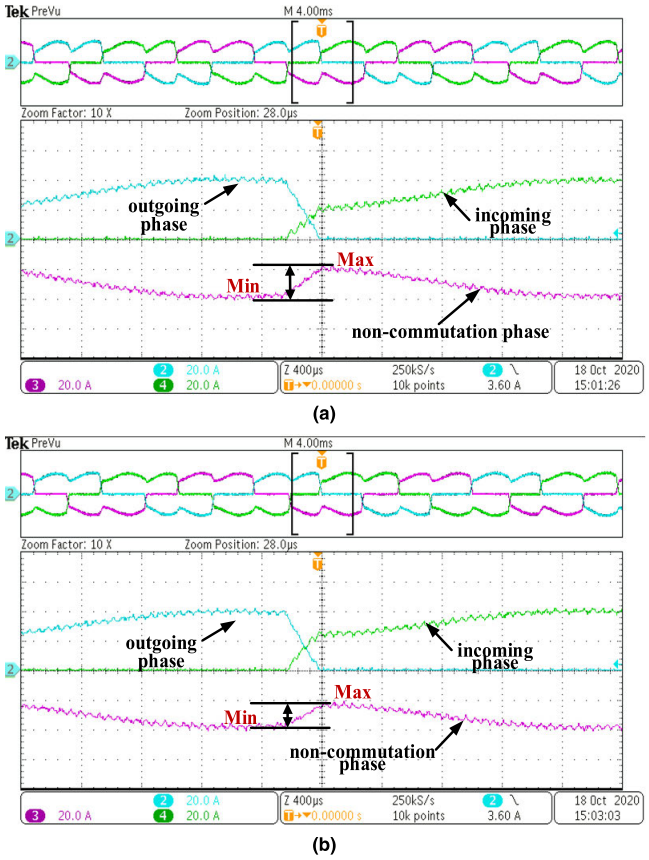

FIGURE 19. Experimental waveform of current under two methods when D = 0.6. (a) ordinary PWM-OFF-PWM. (b) improved PWM-OFF-PWM.

When the duty cycle $D = 0.4$, in order to meet the requirements of $D_{on} + D_{off} = 2(1 - D) = 1.2$ and $D_{off} < D < D_{on}$, the duty cycles of incoming and outgoing phase under the improved PWM-OFF-PWM are selected as $D_{on} = 0.82$ and $D_{off} = 0.38$ respectively.

When the duty cycle $D = 0.4$, the three-phase current waveforms under the ordinary and improved PWM-OFF-PWM method are shown in Fig.18 (a) and (b), separately.

Comparing Fig.18 (a) and (b), it can be found that compared with the ordinary PWM-OFF-PWM method, the non-commutation current fluctuation is reduced, indicating that the improved PWM-OFF-PWM can effectively suppress the commutation torque ripple.

2) $D = 0.5$

When the duty cycle $D = 0.5$, in order to meet the requirements of $D_{on} + D_{off} = 2(1 - D) = 1$ and $D_{off} < D < D_{on}$, the duty cycles of incoming and outgoing phase under the improved method are selected as $D_{on} = 0.9$ and $D_{off} = 0.1$ respectively.

When $D = 0.5$, the experimental current waveform of ordinary and improved PWM-OFF-PWM methods are shown in Fig.14 and Fig.17 respectively. Comparing Fig.14 and Fig.17, it can be found that the improved PWM-OFF-PWM can effectively suppress the commutation torque ripple.

3) $D = 0.6$

When the duty cycle $D = 0.6$, in order to meet the requirements of $D_{on} + D_{off} = 2(1 - D) = 0.8$ and $D_{off} < D < D_{on}$, the duty cycles of incoming and outgoing phase under the improved PWM-OFF-PWM method are selected as $D_{on} = 0.77$ and $D_{off} = 0.03$ respectively. And the three-phase current waveforms under the ordinary and improved PWM-OFF-PWM methods are shown in Fig.19 (a) and (b), separately.

Comparing Fig.19 (a) and (b), it can be found that the improved PWM-OFF-PWM can effectively suppress the commutation torque ripple. Through the current waveforms of the two methods, it can be seen that the improved PWM-OFF-PWM can significantly suppress the pulsation of non-commutation current under different duty cycle D conditions.

Therefore, as long as the duty cycles of the outgoing and the incoming phases are satisfied (22) under different duty cycle D, the phenomenon of non-commutation phase current drop in the commutation region is able to be effectively improved, which verifies that the proposed theory is capable of significantly suppressing commutation torque ripple.

V. CONCLUSION

To suppress commutation torque ripple caused by turn-off time less than turn-on time in PWM-OFF-PWM mode, an improved overlapping commutation method with dynamic adjustable commutation time is proposed in this paper. As long as the duty cycles of outgoing and incoming phases satisfy derived formula, the non-commutation current in commutation interval will be more stable, thus the commutation torque ripple under ordinary PWM-OFF-PWM mode can be suppressed, and the operation stability of BLDCM can be improved.

REFERENCES

[1] D.-K. Kim, K.-W. Lee, and B.-I. Kwon, "Commutation torque ripple reduction in a position sensorless brushless DC motor drive," *IEEE Trans. Power Electron.*, vol. 21, no. 6, pp. 1762–1768, Nov. 2006.

[2] Y. Zhou, D. Zhang, X. Chen, and Q. Lin, "Sensorless direct torque control for saliency permanent magnet brushless DC motors," *IEEE Trans. Energy Convers.*, vol. 31, no. 2, pp. 446–454, Jun. 2016.

[3] Y.-K. Lin and Y.-S. Lai, "Pulsewidth modulation technique for BLDCM drives to reduce commutation torque ripple without calculation of commutation time," *IEEE Trans. Ind. Appl.*, vol. 47, no. 4, pp. 1786–1793, Jul. 2011.

[4] Z. Li, Q. Kong, S. Cheng, and J. Liu, "Torque ripple suppression of brushless DC motor drives using an alternating two-phase and three-phase conduction mode," *IET Power Electron.*, vol. 13, no. 8, pp. 1622–1629, Jun. 2020.

[5] K. Liu, Z. Zhou, and W. Hua, "A novel region-refinement pulse width modulation method for torque ripple reduction of brushless DC motors," *IEEE Access*, vol. 7, pp. 5333–5342, Jan. 2019.

[6] K. Xia, Y. Ye, J. Ni, Y. Wang, and P. Xu, "Model predictive control method of torque ripple reduction for BLDC motor," *IEEE Trans. Magn.*, vol. 56, no. 1, pp. 1–6, Jan. 2020.

[7] C. Xia, Y. Wang, and T. Shi, "Implementation of finite-state model predictive control for commutation torque ripple minimization of permanent-magnet brushless DC motor," *IEEE Trans. Ind. Electron.*, vol. 60, no. 3, pp. 896–905, Mar. 2013.

[8] J.-H. Song and I. Choy, "Commutation torque ripple reduction in brushless DC motor drives using a single DC current sensor," *IEEE Trans. Power Electron.*, vol. 19, no. 2, pp. 312–319, Mar. 2004.

[9] W. Jiang, P. Wang, Y. Ni, J. Wang, L. Wang, and Y. Liao, "Multimode current hysteresis control for brushless DC motor in motor and generator state with commutation torque ripple reduction," *IEEE Trans. Ind. Electron.*, vol. 65, no. 4, pp. 2975–2985, Apr. 2018.
[10] T. Shi, Y. Guo, P. Song, and C. Xia, "A new approach of minimizing commutation torque ripple for brushless DC motor based on DC–DC converter," *IEEE Trans. Ind. Electron.*, vol. 57, no. 10, pp. 3483–3490, Oct. 2010.
[11] V. Viswanathan and J. Seenithangom, "Commutation torque ripple reduction in the BLDC motor using modified SEPIC and three-level NPC inverter," *IEEE Trans. Power Electron.*, vol. 33, no. 1, pp. 535–546, Jan. 2018.
[12] W. Chen, Y. Liu, X. Li, T. Shi, and C. Xia, "A novel method of reducing commutation torque ripple for brushless DC motor based on cuk converter," *IEEE Trans. Power Electron.*, vol. 32, no. 7, pp. 5497–5508, Jul. 2017.
[13] X. Li, C. Xia, Y. Cao, W. Chen, and T. Shi, "Commutation torque ripple reduction strategy of Z-source inverter fed brushless DC motor," *IEEE Trans. Power Electron.*, vol. 31, no. 11, pp. 7677–7690, Nov. 2016.
[14] X. Yao, J. Zhao, J. Wang, S. Huang, and Y. Jiang, "Commutation torque ripple reduction for brushless DC motor based on an auxiliary step-up circuit," *IEEE Access*, vol. 7, pp. 138721–138731, Oct. 2019.
[15] T. Shi, Y. Cao, G. Jiang, X. Li, and C. Xia, "A torque control strategy for torque ripple reduction of brushless DC motor with nonideal back electromotive force," *IEEE Trans. Ind. Electron.*, vol. 64, no. 6, pp. 4423–4433, Jun. 2017.
[16] T. Sheng, X. Wang, J. Zhang, and Z. Deng, "Torque-ripple mitigation for brushless DC machine drive system using one-cycle average torque control," *IEEE Trans. Ind. Electron.*, vol. 62, no. 4, pp. 2114–2122, Apr. 2015.
[17] Y. Liu, Z. Q. Zhu, and D. Howe, "Instantaneous torque estimation in sensorless Direct-Torque-Controlled brushless DC motors," *IEEE Trans. Ind. Appl.*, vol. 42, no. 5, pp. 1275–1283, Sep. 2006.
[18] Y. Liu, Z. Q. Zhu, and D. Howe, "Commutation-torque-ripple minimization in direct-torque-controlled PM brushless DC drives," *IEEE Trans. Ind. Appl.*, vol. 43, no. 4, pp. 1012–1021, 2007.
[19] C. K. Lad and R. Chudamani, "Simple overlap angle control strategy for commutation torque ripple minimisation in BLDC motor drive," *IET Electr. Power Appl.*, vol. 12, no. 6, pp. 797–807, Jul. 2018.
[20] W. Jiang, Y. Liao, J. Wang, P. Wang, and Y. Xie, "Improved control of BLDCM considering commutation torque ripple and commutation time in full speed range," *IEEE Trans. Power Electron.*, vol. 33, no. 5, pp. 4249–4260, May 2018.
[21] J. W. Dixon and M. E. Ortuzar, "Ultracapacitors + DC-DC converters in regenerative braking system," *IEEE Aerosp. Electron. Syst. Mag.*, vol. 17, no. 8, pp. 16–21, Aug. 2002.
[22] T. Shi, H. Lu, Y. Cao, X. Li, and C. Xia, "Supercapacitor/battery hybrid energy storage unit for brushless DC motor operation," *IET Electr. Power Appl.*, vol. 14, no. 4, pp. 597–604, Apr. 2020.
[23] Y. Cao, T. Shi, Y. Yan, X. Li, and C. Xia, "Braking torque control strategy for brushless DC motor with a noninductive hybrid energy storage topology," *IEEE Trans. Power Electron.*, vol. 35, no. 8, pp. 8417–8428, Aug. 2020.
[24] M.-J. Yang, H.-L. Jhou, B.-Y. Ma, and K.-K. Shyu, "A cost-effective method of electric brake with energy regeneration for electric vehicles," *IEEE Trans. Ind. Electron.*, vol. 56, no. 6, pp. 2203–2212, Jun. 2009.
[25] T. Shi, X. Niu, W. Chen, and C. Xia, "Commutation torque ripple reduction of brushless DC motor in braking operation," *IEEE Trans. Power Electron.*, vol. 33, no. 2, pp. 1463–1475, Feb. 2018.
[26] X. Nian, F. Peng, and H. Zhang, "Regenerative braking system of electric vehicle driven by brushless DC motor," *IEEE Trans. Ind. Electron.*, vol. 61, no. 10, pp. 5798–5808, Oct. 2014.
[27] Y. Cao, T. Shi, X. Niu, X. Li, and C. Xia, "A smooth torque control strategy for brushless DC motor in braking operation," *IEEE Trans. Energy Convers.*, vol. 33, no. 3, pp. 1443–1452, Sep. 2018.
[28] X. Zhou and J. Fang, "Precise braking torque control for attitude control flywheel with small inductance brushless DC motor," *IEEE Trans. Power Electron.*, vol. 28, no. 11, pp. 5380–5390, Nov. 2013.
[29] W.-C. Chi, M.-Y. Cheng, and C.-H. Chen, "Position-sensorless method for electric braking commutation of brushless DC machines," *IET Electr. Power Appl.*, vol. 7, no. 9, pp. 701–713, Nov. 2013.
[30] X. L. Yao, Y. Zhang, and X. M. Jiang, "A novel PWM-OFF-PWM mode for braking operation of brushless DC motor," in *Proc. IECON*, Beijing, China, Dec. 2017, pp. 1711–1716.
[31] C. Bian, C. Chen, Z. Zhang, Y. Man, Z. Wu, and X. Li, "Research on regenerative braking torque ripple suppression of brushless DC motor," in *Proc. 22nd Int. Conf. Electr. Mach. Syst. (ICEMS)*, Harbin, China, Aug. 2019, pp. 1–5.

QIXUN ZHOU was born in Hunan, China, in 1979. He received the B.S. degree in science from the Xi'an University of Technology, in 2001, the M.E. degree, in 2004, and the Ph.D. degree in mechanical engineering from Northwestern Polytechnical University, in 2012. From 2013 to 2017, he was a Postdoctoral Researcher with the School of Mechanical and Electrical Engineering, Northwestern Polytechnical University. He currently works with the School of Electrical and Control Engineering, Xi'an University of Science and Technology. His current research interest includes research on control technology of permanent magnet synchronous motor.

JIANHUA SHU was born in Shaanxi, China, in 1997. She received the B.S. degree in electrical engineering from the Xi'an University of Science and Technology, Xi'an, China, in 2019, where she is currently pursuing the M.S. degree in electrical engineering with the School of Electrical and Control Engineering. Her current research interest includes commutation ripple suppression of BLDCM.

ZIWEI CAI was born in Shaanxi, in 1997. She received the B.S. degree in automation engineering from the Xi'an University of Science and Technology, in 2019, where she is currently pursuing the M.S. degree in electrical engineering with the School of Electrical and Control Engineering. Her current research interest includes control technology of permanent magnet synchronous motor.

QUANLONG LIU received the B.S. degree in electrical engineering from the Xi'an University of Science and Technology, in 2018, where he is currently pursuing the M.S. degree in electrical engineering with the School of Electrical and Control Engineering. His current research interests include control technology of permanent magnet synchronous motor and predictive control technology.

GUANGHUI DU was born in Henan, China, in 1987. He received the B.S. degree in electrical engineering from Qingdao Agricultural University, China, in 2010, and the Ph.D. degree in electrical engineering from the Shenyang University of Technology, in 2015. From 2016 to 2017, he worked with CRRC Yongji Electric Company Ltd. He joined the School of Electronics and Information Engineering, Xi'an Technological University, in 2017. From 2018 to 2019, he worked as a Postdoctoral Research Fellow with the School of Electrical and Electronic Engineering, Huazhong University of Science and Technology. He currently works with the School of Electrical and Control Engineering, Xi'an University of Science and Technology. His current research interests include design of high-speed machines and permanent magnet machines.